Carpathian Journal of Earth and Environmental Sciences, August 2018, Vol. 13, No. 2, p. 575 - 593; DOI:10.26471/cjees/2018/013/049

THE CHARACTERISTICS AND EVOLUTION OF DIAGENESIS IN A HIGH-RESOLUTION SEQUENCE STRATIGRAPHICAL FRAMEWORK OF SANDSTONE RESERVOIR - IN THE TOUTUNHE FORMATION IN THE FUDONG SLOPE AREA，JUNGGAR BASIN, CHINA

Jingwei YU[1] Zesheng WANG[2] Juan YU[2], Kunlin XUE[3], Liqi QI[1] & Huaguo WEN[4]

[1]Karamay Campus of China University of Petroleum Xinjiang Karamay 834000; 2. CNPC xinjiang oilfield Exploration and Development Research Institution, Xinjiang Karamay 834000;3. CNPC xinjiang oilfield oil production plant of Baikouquan, Xinjiang Karamay 834000;4.Chengdu University of Technology Chengdu 610059;e-mail:yyjjww-1985@163.com

Abstract: Most favorable area of target reservoirs in Fudong area of Junggar Basin has been predicted only by means of high-resolution sequence stratigraphy or diagenesis evolution, which could not satisfy precise exploration requirement. However, the coupling of high-resolution sequence stratigraphy and diagenesis evolution can not only divide thin sand layer, but also supply diagenetic anisotropy in thin sand layer, all of which has poster significance in the exploration of hydrocarbons. Therefore, on the basis of previous research on sequence stratigraphy, the characteristics and evolution of diagenesis in a high-resolution sequence stratigraphical framework of reservoir sand in the Toutunhe Formation in the Fudong slope area are analyzed by using drilling and logging data as well as extensive experimental data in this work. The results indicate that the sequence of the interface is able to control the contact relationship between grains, the content of rock fragments, the content of feldspar, the content of cements and the transformation between clay minerals. Four structural types of the short-term cycle exist, and this research discusses the character of diagenesis within different structural types of short-term cycles. This research reflects that sequence stratigraphy has a certain relationship with diagenesis. The analysis of diagenesis evolution in cycles with different structural types is able to provide guidance on how to find productive reservoirs in small area regions.

Keywords: High-resolution sequence stratigraphy; Diagenesis character; Diagenesis evolution; Fudong slope area

1. INTRODUCTION

The Junggar Basin is one of the large superimposed basins in China. It can be divided into eight structural zones (Lu et al., 2008; Yu, 2015) according to the basement and tectonic features of the basin. The Fukang Depression located in the depression zone in the southern part of the basin (Fig. 1) is a secondary structural unit, which is rich in source rocks and less structurally influenced. In the slope belt in the east of the basin, oil and gas resources are relatively abundant and have been well explored. Hydrocarbon exploration began in this region in the 1950s. Since then, discoveries have increasingly emerged with improving exploration technologies. Subsequently, the Toutunhe play found between 2010 and 2012 has provided a sound foundation for a commercial increase in hydrocarbon production. In the Middle Jurassic Toutunhe Formation, braided stream deltaic sedimentary systems occurred (Yu et al., 2014), and the extensively distributed sandstones are well collocated with the Jurassic and Permian source rocks, forming an excellent oil reservoir. These characteristics are favorable for the formation of a vast play with a great potential.

In response to the oil and gas exploration situation around the world, the current efforts on the play are mostly focused on exploration of the Jurassic lithologic traps in the Fudong Slope Belt. In fact, in the Fudong Slope Belt near the oil-generating depression, the extensively distributed Jurassic sand bodies are in close contact with the source rocks via unconformities

and faults that act as effective pathways for hydrocarbon migration, having a great potential to form a series of lithologic traps. These issues are the focuses of this work. The previous predictions of the Jurassic lithologic traps in the study area were performed based on stratigraphic sequence and sedimentary facies studies (Yu, 2015), and these studies paid more attention to the existing excellent reservoir volumes than their formation processes, resulting in inaccurate prediction results.

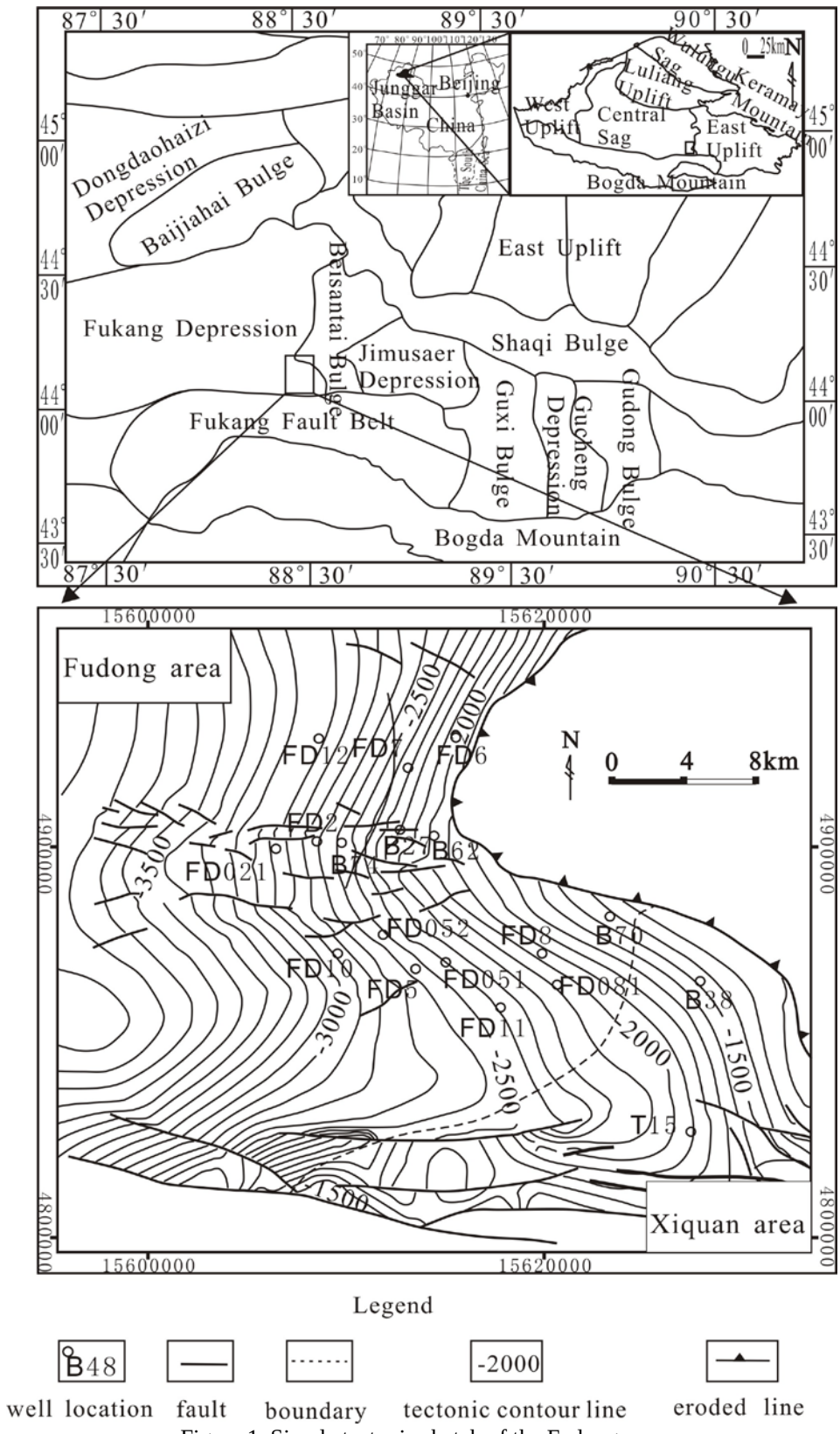

Figure 1. Simple tectonic sketch of the Fudong area

The formation of an excellent reservoir volume is generally caused by two processes. The first process is deposition of the sediments that may last for a time much shorter than the second process, diagenesis (Soreghan et al., 2005; Morad et al., 2010). Owing to the introduction of sequence stratigraphy, especially the theory of high-resolution sequence stratigraphy, the deposition of an excellent reservoir volume can be studied within a sequence stratigraphical framework more accurately than before, providing a basis for rough prediction of subtle reservoirs (Soreghan et al., 2005; Fernando et al., 2015; Ahmed et al., 2016; Hilda et al., 2017). However, previous studies on the diagenesis crucial to formation of an excellent reservoir often dealt with descriptions of diagenetic types and their evolutions (Cao et al., 2015; Cao et al., 2016; Andrew, 2015; Alexandre et al., 2016; Álvaro et al., 2017). The failure to integrate with the sequence stratigraphy, especially the high-resolution sequence stratigraphy, and negligence of the short-time-scale diagenetic process of the reservoir volume resulted in failure to observe the temporal and spatial distributions of diagenesis of the reservoir volume. This result is unfavorable for accurate prediction of the distribution of the excellent reservoir volume.

By combining sequence stratigraphy and diagenesis, various researchers have proposed new approaches for fine prediction of excellent reservoirs. Liu et al. (2014) reviewed research on the macroscopic heterogeneities of the reservoirs using high-resolution sequence stratigraphy. However, it emphasizes macroscopic heterogeneity in middle-term cycles (equivalent to the Grade Ⅳ sequence derived by Vail et al., (1991), which is not precise enough in the exploration of hydrocarbons. By using various available data, Higgs et al. (2012) conducted a diagenetic study within multi-scale sequence stratigraphic frameworks, improving the accuracy in prediction of reservoir volumes. Although they used multi-scale sequence stratigraphy and diagenetic study to predict favorable reservoir, the type of cyclic structures is neglected and it could not show relationship between diagenetic and types of cyclic structures. Morad et al. (2010) summarized the controls of the sequence stratigraphy over the diagenesis and heterogeneities of clastic rocks. But they neglected how to combine diagenesis with the sequence stratigraphy to predict reservoir volumes. In summary, the combination of short-time-scale sequence stratigraphy and diagenesis to guide the prediction of reservoir volumes represents a leading research focus in the future (Zhang et al., 2016).

In this work, an approach for reservoir prediction is proposed that is the combination of short-time-scale sequence stratigraphy and diagenesis on the basis of previous studies. This approach first is to establish short-time-scale sequence stratigraphic framework, which needs to satisfy precise exploration of hydrocarbons. Then it is to build relationship between low grade sequence boundary and diagenesis, which is to investigate the controls of the sequence stratigraphy over the diagenesis. At last, it is to discuss the evolution and difference in diagenesis for various types of cyclic structures, predict reservoir volumes in target formation. This work studies about the evolution and difference in diagenesis for various types of cyclic structures under short-time-scale sequence stratigraphic framework for Toutunhe Formation in Fudong area of Junggar Basin. This is because high-resolution sequence stratigraphy and diagenesis in the target formation has been studied, but how to combine high-resolution sequence stratigraphy with diagenesis to predict reservoir volumes have not been studied. This work studied diagenetic evolutions within different middle-term cycles and discussed the diagenetic characteristics in various types of cyclic structures at different datum levels and their influences on reservoir potential for the first time. This work can improve the accuracy in the prediction of reservoir volumes and can provide reference for the exploration of lithologic reservoir volumes in similar areas.

2. EXPERIMENTAL

2.1. Geological setting of the study area

The study area is located in the central south portion of the Fudong Slope Belt, situated in the southeastern part of the Junggar Basin and in the north part of the east Tianshan Mountain, the southern margin of the Junggar Basin and the eastern part of the Changji Hui Autonomous Prefecture (Fig. 1). It is east of Fukang City and west of Jimsar country. The whole study area is in a simple structure, with a regional width of 20-40 km and a total area of about 600 km^2. To date, a total of 76 wells have been drilled in the Toutunhe Formation.

By using outcrop, core, logging, well logging and seismic data, the Middle Jurassic Toutunhe Formation in the study area was previously divided in terms of sequence stratigraphy into one long-term cycle (equivalent to the Grade Ⅲ sequence derived by Vail et al., (1991), three middle-term cycles (equivalent to the Grade Ⅳ sequence derived by Vail et al., (1991) and ten short-term cycles (equivalent to the Grade Ⅵ sequence derived by Vail et al., (1991) (Fig. 2) (Qi et al., 2014). The lack of further analysis on the diagenetic characteristics and model of evolution in the Toutunhe Formation within a sequence stratigraphic

framework resulted in inaccurate prediction of the Jurassic lithologic reservoirs and suspension of the exploration process. Therefore, in this paper, differences in diagenetic characteristics and evolution and their influences on the reservoir potential in different sequences of the Toutunhe Formation within a low-grade sequence stratigraphic framework are studied by analyzing logging and laboratory data.

2.2 Samples and Experimental methods

A total of 226 samples of the Toutunhe Formation were cored from 19 wells with even distribution in the study area. All sampling well locations are shown in Figure 1. Among all the samples, 46 were from Member 1 of the Toutunhe Formation, 140 were from Member 2, and 20 were from Member 3. All sample distributions are summarized in Table 1. Experiment and Testing Institute of the Xinjiang Oilfield also supplied data, such as the well logging and seismic data, to support this research.

2.2.1 Mercury injection experiments

The mercury injection experiments were performed on 65 core samples with a diameter of 2.5 cm and a length of 2.0 cm using a PM33GT-17 mercury injection apparatus developed by Quantachrome in the United States. The apparatus has a high-pressure hydraulic system composed of a high-pressure metering pump, with a working pressure range of 0.002-50 MPa. It takes ≥60 s to reach the state of pressure balance and can measure 100 pressure points. The experiments were performed by the Experiment and Testing Institute of the Xinjiang Oilfield in accordance with standard SY/T5346-2005 for the Approach for Measurement of Capillary Pressure Curve of a Rock. The results are shown in Table 2.

2.2.2 Preparation of conventional thin sections and cast thin sections

In accordance with the standard SY-5913-2004, a total of 153 samples of 25mm×5mm size have been prepared by cutting, washing with oil, casting with glue (with a 6 MPa pressure), cementing with glue and smoothing by the Experiment and Testing Institute of the Xinjiang Oilfield.

2.2.3 SEM and X diffraction analyses

The samples in a range of 10-15 mm in diameter and 5 mm in length were analyzed under SEM with an electron beam of 10.9 mA and a voltage as high as 5 kV. In accordance with standard SY/T5162-1997 for the Approach for Analysis of the Rock Samples under

Table 1 Samples distribution in 20 wells

well	Sample distribution			Mercury injection			thin and cast thin sections			SEM	XRD	
	Member 1	Member 2	Member 3	Member 1	Member 2	Member 3	Member 1	Member 2	Member 3	Member 2	Member 1	Member 2
B27	11	6	2				3	6	1	1	4	6
B36	6	7	3				3	7	1	2	2	7
B38		8						8		1		8
B70		5	5					5	1	3		5
B62		8						8				8
B74		8						8				8
FD021		5						5		2		5
FD051	7	5		3			4	5		2	2	5
FD052		12			12			12		3		8
FD081	17	10		13	7		3	10		3	4	8
FD10		5						5		5		5
FD11		7						7		3		7
FD12		11			12			5		2		11
FD2		12	7		12	3		7	3	3		6
FD5		10						7		4		5
FD6		10						5		4		10
FD7		19	3		1			10	1	6		5
FD8	5	1		2			2	1		1	3	1
T15		11						11				11

Table 2. 69 results of mercury injection experiments

No.	well	depth	formation	Pore volume	Pore	Perm	mean	Sorting coefficient	skewness	kurtosis	Variable coefficient	Median pressure	Median radius	Entry pressure	maximal radiuses of pore throats	mercury withdrawal efficiency	porethroat volume ratio	Average capillary radius	uniformity coefficient	Pore volume percent
1	FD081	2614.43	J2t2	1.88	15.9	1.37	11.43	1.99	0.04	1.32	0.17	3.28	0.22	0.67	1.09	22.38	3.47	0.48	0.3	32.92
2	FD081	2615.23	J2t2	1.96	16.4	1.81	11.24	2	0.18	1.36	0.18	2.37	0.31	0.65	1.14	14.37	5.96	0.52	0.33	29.94
3	FD081	2656.78	J2t2	2.47	21.9	318	8.14	3.2	0.78	2.09	0.39	0.14	5.14	0.04	16.85	7.19	12.91	7.46	0.32	16.83
4	FD081	2656.99	J2t2	2.26	21.8	230	10.19	3.19	-0.09	1.42	0.31	1.25	0.59	0.07	10.88	16.44	5.08	3.28	0.17	35.32
5	FD081	2657.26	J2t2	2.14	17.8	13.4	10.26	2.64	0.22	1.49	0.26	1.09	0.67	0.16	4.53	11	8.09	1.58	0.23	26.64
6	FD081	2657.96	J2t2	0.51	4.6	0.097	12.1	1.79	-0.68	2.19	0.15	9.15	0.08	0.57	1.28	36.71	1.72	0.31	0.15	40.56
7	FD081	2661.17	J2t2	1.66	15.1	2.87	11.43	2.09	-0.05	1.3	0.18	3.59	0.2	0.55	1.35	18.04	4.54	0.52	0.26	35.78
8	FD081	2708.18	J2t1	2.26	19.9	317	9.34	3.72	0.05	1.31	0.4	0.83	0.89	0.03	23.56	9.49	9.54	7.52	0.19	31.84
9	FD081	2710.51	J2t1	2.28	21.1	43.4	9.34	3.76	0.05	1.28	0.4	0.87	0.84	0.03	23.48	9.49	9.54	7.56	0.19	32.44
10	FD081	2710.55	J2t1	1.91	21.4	未测	8.99	3.47	0.33	1.49	0.39	0.41	1.78	0.04	19.13	6.98	13.33	6.33	0.21	26.14
11	FD081	2710.94	J2t1	2.38	20.1	85.1	9.39	3.07	0.08	1.76	0.33	0.83	0.89	0.04	19.82	12.1	7.26	4.78	0.13	17.9
12	FD081	2711.59	J2t1	2.54	21.5	65	9.58	2.87	0.26	1.7	0.3	0.69	1.06	0.07	10.98	8.18	11.22	3.11	0.17	19.93
13	FD081	2712.87	J2t1	2.57	22.3	52.1	10.92	2.92	-0.47	1.73	0.27	5.1	0.14	0.08	8.83	11.54	7.67	2.09	0.12	35.16
14	FD081	2713.48	J2t1	2.22	19.1	17.5	10.85	2.45	0.06	1.31	0.23	1.99	0.37	0.29	2.55	16.91	4.92	0.98	0.26	31.33
15	FD081	2742.25	J2t1	1.84	15.6	2.73	11.38	1.98	0.08	1.34	0.17	2.94	0.25	0.67	1.09	22.38	3.47	0.48	0.31	31.47
16	FD081	2745.55	J2t1	1.85	15.5	0.655	12.12	1.74	-0.57	1.98	0.14	9.41	0.08	0.74	0.99	24.52	3.08	0.26	0.17	41.29
17	FD081	2746.55	J2t1	1.9	16	3.02	11.45	1.99	0.01	1.31	0.17	3.45	0.21	0.68	1.09	22.38	3.47	0.47	0.3	33.63
18	FD081	2748	J2t1	2.07	17.1	2.53	11.74	2.03	-0.6	2.11	0.17	7.07	0.1	0.37	1.97	18.61	4.37	0.48	0.14	33.96
19	FD081	2749.64	J2t1	2.05	18	2.42	11.14	2.22	0.05	1.44	0.2	2.16	0.34	0.35	2.08	11.53	7.67	0.63	0.21	34.54
20	FD081	2760.68	J2t1	1.88	16.4	3.91	11.41	2.01	0.03	1.33	0.18	3.28	0.22	0.65	1.13	22.38	3.47	0.49	0.3	32.92
21	FD052	2972.51	J2t2	1.02	9.1	0.795	11.36	1.96	0.04	1.45	0.17	3.16	0.23	0.58	1.27	29.56	2.38	0.48	0.26	30.14

22	FD052	2973.27	J2t2	1.07	9.5	5.39	12.78	1.18	-0.78	2.15	0.09	18.91	0.04	2.22	0.33	33.05	2.03	0.11	0.25	48.53
23	FD052	2973.61	J2t2	1.07	9.7	0.084	12.76	1.16	-0.69	2	0.09	17.17	0.04	2.51	0.29	43.87	1.28	0.11	0.28	46.82
24	FD052	2973.9	J2t2	1.31	11.6	0.205	12.76	1.19	-0.71	2	0.09	17.83	0.04	2.32	0.32	37.25	1.68	0.12	0.26	47.4
25	FD052	2974.02	J2t2	1.23	11.1	0.113	12.69	1.19	-0.61	1.88	0.09	14.73	0.05	2.25	0.33	37.25	1.68	0.12	0.27	43.98
26	FD052	3027.08	J2t2	1.56	13.6	0.21	12.21	1.39	-0.36	1.98	0.11	7.27	0.1	1.27	0.58	27.74	2.6	0.18	0.23	30.65
27	FD052	3045.81	J2t2	0.75	6.3	0.419	11.74	1.91	-0.23	1.54	0.16	4.85	0.15	0.59	1.24	28.98	2.45	0.38	0.2	37.63
28	FD052	3046.39	J2t2	2.08	17.9	18.88	9.45	2.66	0.69	1.83	0.28	0.47	1.58	0.16	4.5	7	13.28	2.21	0.37	19
29	FD052	3047.05	J2t2	1.75	17.4	14.9	10.33	2.77	0.16	1.34	0.27	1.07	0.68	0.17	4.39	10.48	8.54	1.69	0.25	30.58
30	FD052	3047.31	J2t2	1.98	17.9	15.11	9.61	2.77	0.53	1.62	0.29	0.52	1.41	0.14	5.43	15.44	5.48	2.26	0.3	21.99
31	FD052	3047.73	J2t2	1.68	14.6	2.52	11.34	2.37	-0.24	1.38	0.21	4.99	0.15	0.34	2.14	15.36	5.51	0.76	0.22	38.27
32	FD052	3048.09	J2t2	0.87	7.8	1.39	12.02	1.91	-0.48	1.66	0.16	12.44	0.06	0.64	1.15	28.98	2.45	0.34	0.19	46.23
33	FD12	3300.72	J2t2	1.14	10.2	0.053	13.38	0.7	-1.97	5.74	0.05	0	0	4.62	0.16	27.62	2.62	0.05	0.26	62.1
34	FD12	3301.84	J2t2	1.8	16.5	35.55	10.5	3.14	-0.27	1.46	0.3	2.41	0.3	0.09	8.44	11.71	7.54	2.93	0.19	37.29
35	FD12	3312.08	J2t2	1.41	12.9	16.99	11.15	2.28	-0.35	1.95	0.2	3.55	0.21	0.21	3.55	14.91	5.71	0.83	0.13	26.2
36	FD12	3312.98	J2t2	1.96	20.2	81.33	9.8	3.07	0.05	1.45	0.31	1.13	0.65	0.08	9.12	10.38	8.63	3.52	0.23	23.99
37	FD12	3313.92	J2t2	2.08	19.2	51.99	9.51	3.02	0.18	1.52	0.32	0.91	0.8	0.08	9.6	10.88	8.19	3.77	0.25	19.01
38	FD12	3314.76	J2t2	1.03	9.2	3.75	10.2	2.26	0.52	1.72	0.22	1.01	0.72	0.28	2.59	12.78	6.82	1.12	0.32	17.84
39	FD12	3315.5	J2t2	2.21	21.2	39.2	10.17	2.84	-0.1	1.6	0.28	1.82	0.4	0.09	8.25	15.15	5.6	2.51	0.17	22.34
40	FD12	3316.49	J2t2	1.28	11.7	8.76	9.9	2.41	0.48	1.88	0.24	0.76	0.96	0.14	5.2	10.72	8.33	1.51	0.2	16.8
41	FD12	3317.12	J2t2	1.09	9.7	3.93	10.55	2.24	0.32	1.58	0.21	1.25	0.59	0.3	2.43	14.36	5.96	0.94	0.27	21.29
42	FD12	3317.79	J2t2	1.78	17.7	77	9.3	3.14	0.32	1.5	0.34	0.6	1.23	0.07	10.41	8.91	10.23	4.19	0.27	21.71
43	FD12	3318.43	J2t2	1.64	16.5	65.55	8.52	2.63	0.9	2.53	0.31	0.29	2.49	0.07	9.84	6.57	14.21	4.03	0.3	10.61
44	FD12	3319.25	J2t2	0.32	2.8	0.146	12.76	1.51	-1.1	2.57	0.12	0	0	1.28	0.58	59.52	0.68	0.17	0.18	62.74
45	FD2	3115.32	J2t3	1.05	9.4	1.29	10.96	2.11	0.14	1.6	0.19	2.09	0.35	0.35	2.1	26.29	2.8	0.66	0.22	25.07
46	FD2	3149.82	J2t3	0.81	6.9	1.42	10.34	2.17	0.18	2.04	0.21	1.37	0.54	0.18	3.98	53.52	0.87	1.11	0.18	14.16

47	FD2	3150.34	J2t3	1.34	11.7	0.235	12.35	1.48	-0.6	2.08	0.12	9.62	0.08	1.1	0.67	38.14	1.62	0.19	0.19	39.32
48	FD2	3177.55	J2t2	2.19	19.1	93.8	9.42	3.04	0.22	1.52	0.32	0.74	0.99	0.07	10.83	14.55	5.87	3.9	0.23	18.63
49	FD2	3178.09	J2t2	2.05	18	90.4	9.53	3.31	0.18	1.33	0.35	0.76	0.97	0.07	10.69	8.12	11.32	4.23	0.26	27.18
50	FD2	3178.43	J2t2	1.04	9.3	0.904	11.39	2.17	-0.35	1.82	0.19	4.23	0.17	0.27	2.71	24.52	3.08	0.67	0.14	31.71
51	FD2	3178.68	J2t2	2.34	20.2	239	8.59	3.56	0.48	1.5	0.41	0.15	4.89	0.04	16.9	8.76	10.42	7.65	0.31	22.95
52	FD2	3179.43	J2t2	0.56	4.7	0.226	11.43	1.76	0.08	1.7	0.15	3.02	0.24	0.63	1.17	37.26	1.68	0.38	0.23	25.03
53	FD2	3180.86	J2t2	0.94	9.8	7.15	9.95	2.48	0.15	2.05	0.25	1.09	0.68	0.09	7.74	37.5	1.67	1.89	0.15	15.36
54	FD2	3182.35	J2t2	0.68	5.7	1.36	10.55	2.21	0.03	2.01	0.21	1.79	0.41	0.17	4.21	45.24	1.21	1.04	0.15	17.67
55	FD2	3193.5	J2t2	1.87	16.4	54.1	9.13	3.36	0.15	1.65	0.37	0.56	1.31	0.04	17.43	23.97	3.17	5.33	0.19	20.02
56	FD2	3202.5	J2t2	0.95	10.3	34.2	9.36	3.25	-0.07	1.84	0.35	0.88	0.84	0.04	18.37	33.06	2.02	5.08	0.16	18.28
57	FD2	3231.08	J2t2	1.16	13	0.224	12.67	1.43	-1.01	2.63	0.11	0	0	1.34	0.55	36.48	1.74	0.16	0.18	50.59
58	FD2	3231.44	J2t2	1.3	11.5	0.094	12.7	1.49	-1.08	2.65	0.12	0	0	1.2	0.61	34.12	1.93	0.18	0.17	54.8
59	FD2	3311	J2t2	1.74	15.5	0.514	11.56	2.19	-0.47	1.8	0.19	6.33	0.12	0.31	2.36	28.2	2.55	0.64	0.15	34.33
60	FD8	2581.03	J2t1	1.59	13.9	2.78	10.74	2.49	-0.04	1.51	0.23	2	0.37	0.2	3.72	15.18	5.59	1.18	0.19	27.36
61	FD8	2581.33	J2t1	2	17.1	7.39	10.35	2.93	-0.12	1.51	0.28	1.57	0.47	0.09	8.02	13.42	6.45	2.39	0.17	28.84
62	FD7	2830	J2t2	1.6	13.6	0.313	11.82	1.69	-0.47	2.22	0.14	5.67	0.13	0.55	1.34	37.11	1.69	0.32	0.15	25.33
63	FD051	3053	J2t1	1.47	13.4	14.7	11.01	2.73	-0.56	2.25	0.25	4.42	0.17	0.08	9.14	16.51	5.06	1.22	0.07	33.44
64	FD051	3053.36	J2t1	1.13	10.5	0.455	12.05	2.26	-0.92	2.26	0.19	0	0	0	0	27.03	2.7	0	0	50.65
65	FD051	3053.63	J2t1	1.52	13	0.684	11.15	2.56	-0.51	1.74	0.23	6.33	0.12	0.17	4.36	24.57	3.07	1.27	0.15	24.83

a Scanning Electron Microscope (SEM), a total of 45 samples have been analyzed under SEM by the Experiment and Testing Institute of the Xinjiang Oilfield.

When preparing the samples, each sandstone sample was powdered, evenly distributed in a sample frame and compacted with a glass plate, which was subject to experiment by X-ray spectrometer QUANTAX400 with a voltage of 40 kV and a current of 250 mA and at the temperature of 20℃ and the humidity of 50%, in accordance with the standard SY/T6189-1996 for the Approach for Quantitative Spectroscopy of Minerals in Rocks. For this work, X-ray diffraction analyses have been performed on 144 sandstone samples by the Experiment and Testing Institute of the Xinjiang Oilfield.

2.2.4 Well logging and Seismic data

Well logging data of 20 wells, shown in Figure 1, are provided by Logging Company of the Xinjiang Oilfield. Well logging has been corrected, and its types include Spontaneous Potential (SP), Gamma Ray (GR), and Caliper measurement (CALI).

Seismic data are provided by Exploration and Development Institution of the Xinjiang Oilfield. The area of 3D seismic work (3D seismic profiles or lines) is 800 km^2, which contains the study area. The density of horizon tracing is 5m╳5m with high fidelity (Fig. 3).

3. RESULTS

3.1 High-resolution sequence stratigraphic framework of the Toutunhe Formation

From bottom to top, the Toutunhe Formation in the study area can be divided into the Tou 1, Tou 2 and Tou 3 Members. The top and bottom of Toutunhe Formation were eroded unconformity surface, and these unconformity surfaces were sequence boundary of Long sequence cycle (LSC). These unconformity surfaces were shown large-scale truncation surface in seismic profiles and discontinuous surface in logging curves. The top and bottom of every member were also eroded unconformity surface, and these unconformity surfaces were sequence boundary of Middle sequence cycle (MSC). These unconformity surfaces were shown larger-scale discontinuous surface in logging curves. Sequence boundary of Short sequence cycle (SSC) was only shown base scouring surface in cores. Critical surfaces comprise of sequence boundary, initial flooding surface and maximum flooding surface, and these surfaces have been identified and separated on seismic profiles and logging curves. According to the termination patterns of reflection configuration and continuity and amplitude of vibration, transformation of stacking patterns of sequence sets and lithologic profile, the formation can also be divided into one long-term cycle and three middle-term cycles, which correspond well to the members (divided in accordance with the option for division of stratigraphic units of rocks) and seismic sequences (Fig. 2). MSC1 and MSC3 contain three short-term cycles, and MSC2 contains four short-term cycles. Previous research (Qi et al., 2014; Yu et al., 2014; Yu, 2015) on precision of sequence division are often focused on middle-term cycles (equivalent to the Grade Ⅳ sequence derived by Vail et al., (1991). According to vertical association and cycle characteristics, such as weathering and denudation surface, scour surface, sudden change surface of lithologic character and lithofacies, channel incise, transfer surface between ascending and falling, this work divides mid-term cycle into short-term cycles (equivalent to the Grade Ⅵ sequence derived by Vail et al., (1991).

During deposition of the Tou 1 Member (corresponding to MSC1), the slowly rising lake level allowed an abundant provenance to occur in the Kelameili Mountain in the north of the study area, resulting in a number of NE-SW-trending braided-stream deltas in the study area, but the rising lake level restricted the distribution extent of the deltas (Yu, 2015). At the same time, the Bogda Mountain in the south of the study area was just in the beginning of the uplift stage, which provided a limited provenance for a small extent of a braided river delta in the south of the study area, and no deltaic plains have been found there. During deposition of the Tou 2 Member (MSC2), when the lake level rose to the maximum extent, the presence of the abundant provenances in the southern and northern parts of the study area resulted in depositions of the small-scale deltaic plain sediments and extensive underwater distributary channel sand bodies in the study area, indicative of suspected lake regression with respect to MSC1. During deposition of the Tou 3 Member (MSC3), the Yanshan Movement resulted in an extensive erosion area and a slightly extensive deltaic plain; extensively-distributed delta frontal sand bodies (owing to the provenances and topography) were deposited, indicative of real lake regression with respect to MSC1 and MSC2. In summary, the deposition of the Tou 3 Member (MSC3) was characterized by a large front and small plain.

3.2 Petrologic characteristics of the Toutunhe Formation

In the study area, the reservoir sandstones of the Toutunhe Formation are dominated by fine-grained lithic sandstones and secondarily consist of fine- to medium-grained feldspathic lithic sandstone (Fig. 4a).

The sandstones have a ratio of stable components (such as quartz) to unstable components (such as debris + feldspar) of 0.254, including quartz at about 23.3% and feldspar at 21.8% (Table 1). Of the feldspar, orthose is dominant, with some plagioclase. The debris is dominated by magmatic debris, while sedimentary rocks and metamorphic debris are secondary. The probability curve for grain sizes of the rocks in the study area shows one jump and one suspension (Yu et al., 2014), indicating

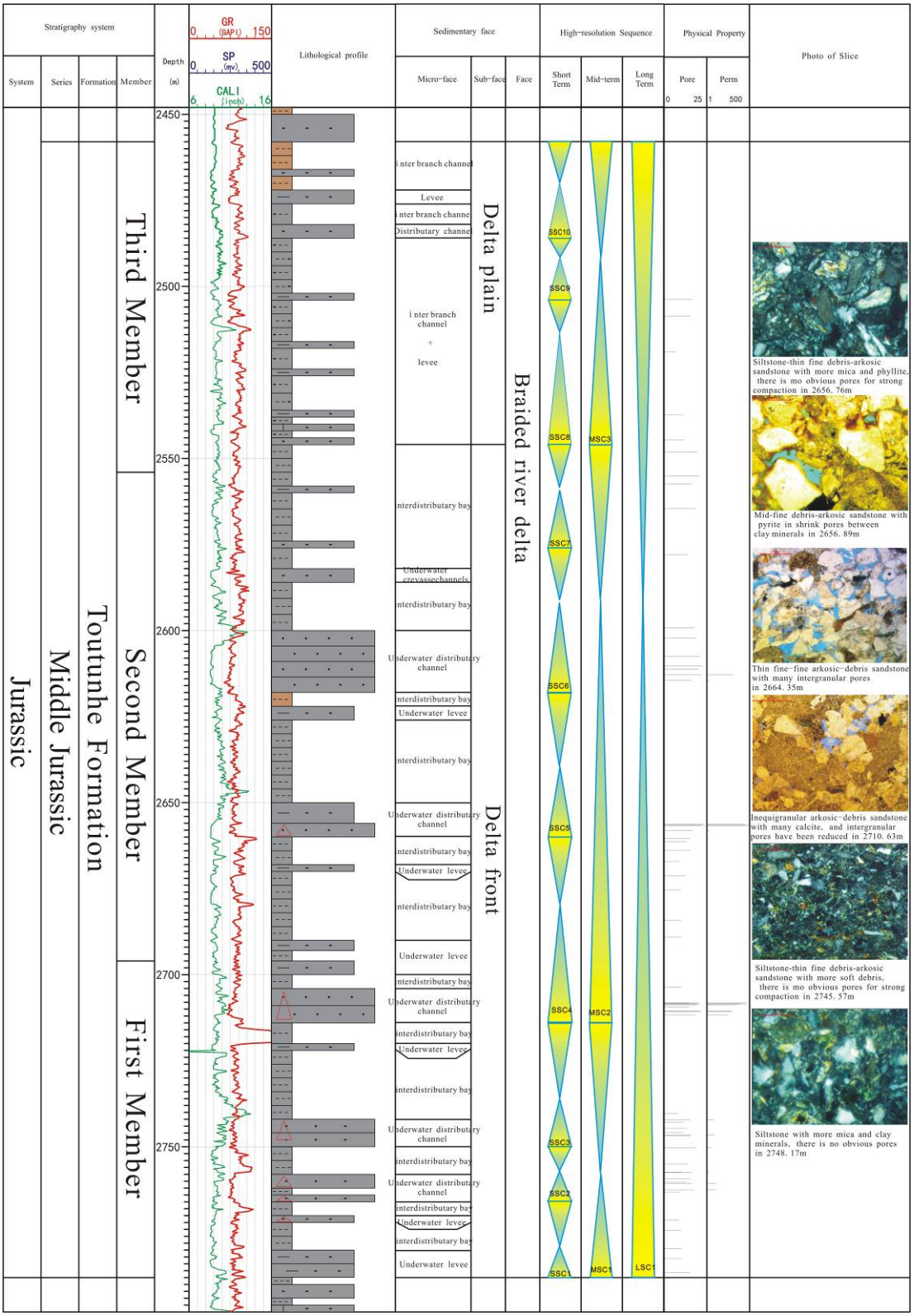

Figure 2. Diagenetic characteristics within a sequence stratigraphic framework of Well Fudong 081 in the study area

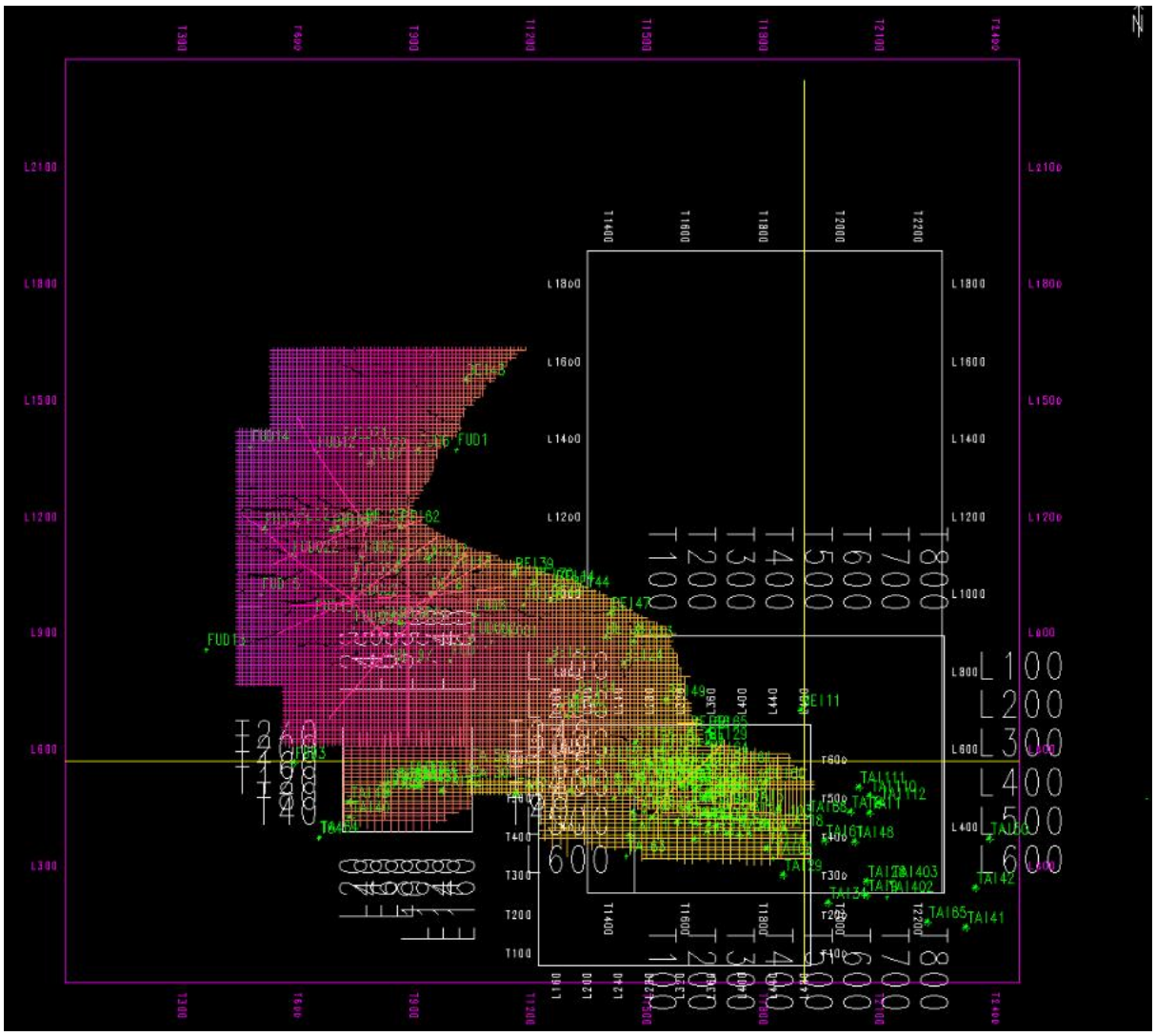

Figure 3. 3D seismic profiles of Toutunhe Formation in Fudong area

Figure 4. Outcrop and cores photos in Toutunhe Formation of the study area

A. Parallel bedding developed in mid-coarse grained sandstone of a Toutunhe Formation profile in Shuimogou； B. Wedge bedding developed in mid-grained sandstone of a Toutunhe Formation profile in Shuimogou； C. Souring structures developed in conglomeratic coarse sand of a Toutunhe Formation profile in Shuimogou； D. Parallel bedding developed in fine-grained sandstone in 2709.63 m of FD081； E. Ripple cross lamination developed in silty mudstone in 3150.47 m of FD2； F. Souring structures developed in conglomeratic coarse sand in 2879.35 m of T15； G. Horizontal bedding developed in mud in 1923.66 m of B79

typical channel sedimentary characteristics. The overall composition maturity is low. The outer shape of the debris is predominantly subangular and is secondarily angular and sub-rounded, with an average sorting coefficient of 2.56, indicating medium to good sorting. The clastic particles are dominantly in point-point contact and locally in point-line contact, which are pore cemented. The matrix content is from 1.12% to 5.94%, having an average of 2.88%, with clay as the dominant substance. The cements are 3.29% - 6.92%, averaged at 4.6%, predominantly consisting of calcareous and siliceous minerals. The secondary overgrowths of quartz and feldspar debris are not obvious, with a generally high structural maturity.

Of the cores from 19 wells, the common primary sedimentary structures consist of parallel bedding, massive bedding, small cross bedding, wavy bedding, horizontal bedding and a bottom scouring surface (Fig. 4). In particular, syngenetic mud gravels often occur at sedimentary boundaries with bottom scouring surfaces. The reservoir spaces in the Toutunhe Formation predominantly consist of primary pores, while intragranular dissolved pores are secondary (Yu, 2015). The petrophysical analysis indicates that the reservoirs of the Toutunhe Formation are porous, with moderate porosities and moderate to low permeabilities (Table 2).

4. DISCUSSION

4.1 Control of the low-grade sequence interface on diagenesis

The Toutunhe Formation in the study area can be divided into 2 III-Grade, 4 IV-Grade and 11V-Grade sequence boundaries (Figs. 2 and 5). These grade-different sequence boundaries are different in the genesis stages. The III-Grade sequence boundaries are related to periodic and episodic changes in intensity of secondary tectonic activity during tectonic evolution; IV-Grade corresponds to datum sea level fluctuation and material supply change as a result of climatic fluctuation in an eccentricity period; and V-Grade relates to datum sea level fluctuation and variation in the A/S ratio (A means Accommodation and S means Sediments supply) as a result of climatic fluctuation in a slope period (Zheng et al., 2001). A sequence boundary refers to an unconformity or relative unconformity at its base or top (Zheng et al., 2001). As identified with well data, particles above a boundary are different in size to those below the boundary, a direct indication of the difference in the sedimentary environment. This difference may be resulted from a diagenetic difference near the boundary (Fig. 2). The control of sequence boundaries over diagenesis has been previously studied. For example, Han (2010) proposed that sequence boundaries may somewhat control dissolution, potentially leading to the dissolution of aluminosilicate near the boundaries and to the presence of kaolinite and secondary pores, indicating that the sequence boundaries may provide paths for fluid to flow. Lai et al., (2014) suggested that sedimentary retention may lead to differences in the degree of compaction below and above the boundaries. For example, carbonate cements below a boundary (about 28%) are higher in content than those above the boundary (less than 9%). The previously discussed sequence boundaries often referred to those corresponding to the III-Grade ones that are Vail (1991) divided. However, in this work, the sequence boundaries are in lower grades corresponding to Vail's (1991) III-Grade or IV-Grade. The diagenetic difference between below and above the boundary may be indicated by thin sections.

(1)Tight interparticle spaces

Previous studies (Yu, 2015; Yu et al., 2015) suggested that the Toutunhe Formation was deposited in an abnormal pressure environment. Due to under-compaction, fluids in the rock pores may bear partial pressure of the overburden sediments, somewhat offsetting the influence of mechanical compaction (Morad et al., 2010). At the boundary, the relatively low residual pressure may allow the rock particles to essentially bear the complete pressure of the overburden sediments. Therefore, particles are in different contacts (Figs. 2 and 5); that is, those particles above the boundary are in point-line contact, while those beneath the boundary are in line-line contact, except for local concave-convex contacts. Due to compaction, some plastic minerals may be squeezed into interparticle pores, somewhat destroying the petrophysical properties of the reservoir sand bodies and poor capacity for hydrocarbon accumulation.

(2)Low-content lithic feldspar

Debris of the Toutunhe Formation is dominated by tuffaceous debris. Due to a relatively low residual pressure near the boundary, the fluid may have a high potential to flow. The flowing fluids may dissolve the tuffaceous debris into feldspar minerals (Mctavish, 1978; Zhu et al., 2011, 2014). The feldspar minerals near the sequence boundary may also be dissolved due to the charging of the atmospheric fresh water and lake water (Figs. 2 and 5). Therefore, the tuffaceous (less than 20%) and feldspar minerals (about 7%) near the boundary are low in content.

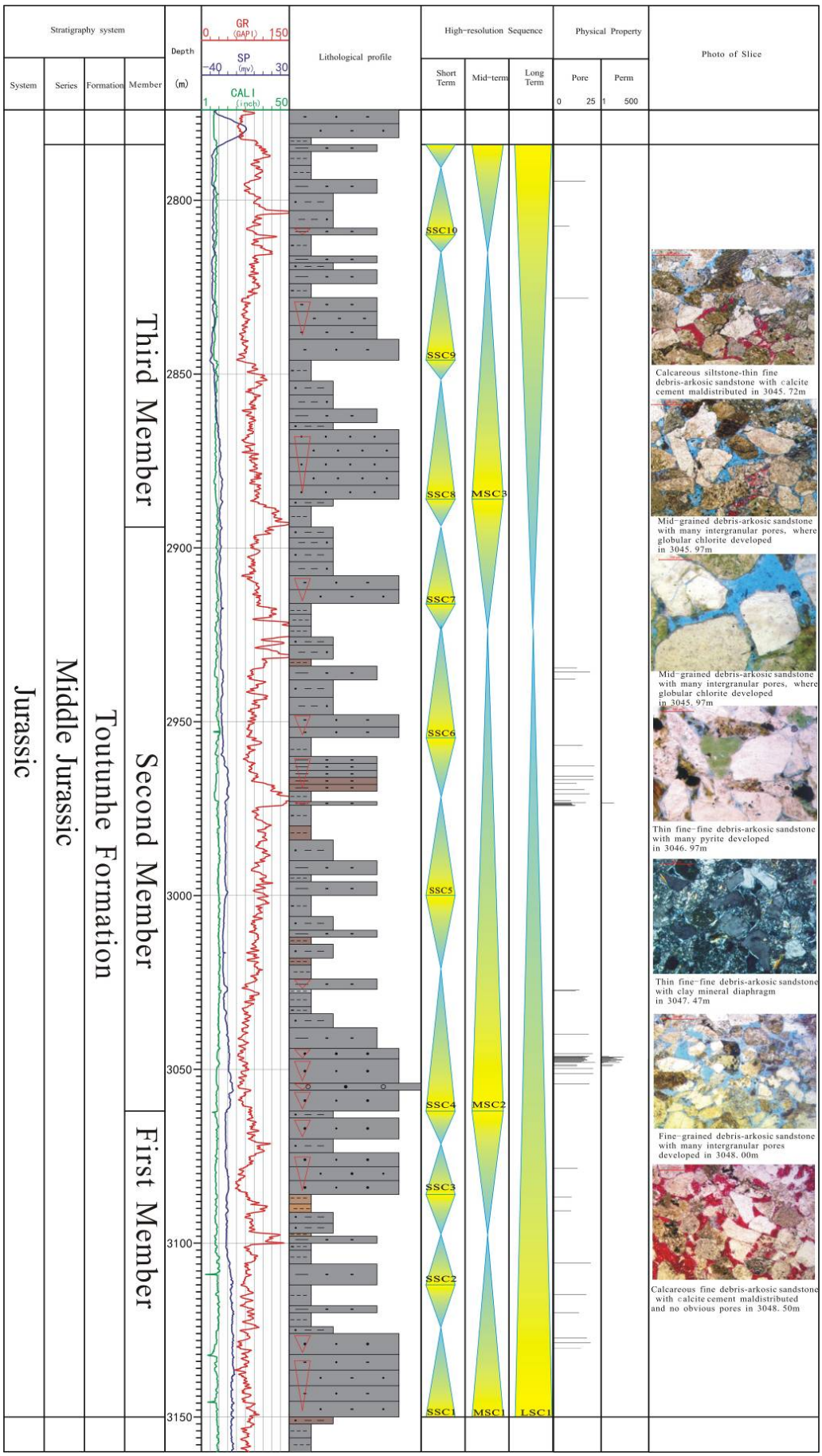

Figure 5. Diagenetic characteristics within a sequence stratigraphic framework of Well Fudong 052 in the study area

(3) High-content cements

Due to the dissolution of the lithic feldspar minerals, alkaline ions, such as K^+, Na^+, Ca^{2+} and Mg^{2+}, are released in large volumes, which may provide an environment conducive to the formation of calcite and zeolite cements around the debris edges below the boundary (Zhu et al., 2011). Due to the high potential of fluid flow at the sequence boundary, the expulsion of a large number of the alkaline ions may lead to weak acidic solution, and transformation of clay minerals and interparticle pre-solution may form Si^{4+} ions. This situation may be conducive to the formation of secondary quartz overgrowths and other siliceous cements in the low residual pressure setting (Fig. 5).

(4) Transformation between clay minerals

The dissolution of lithic feldspar minerals by the high flowing potential fluid may lead to variations in type and content of the clay minerals at the boundary (Figs. 2 and 5). The fluid flow may promote the transformation of the illite-smectite mixture to illite (Zhu et al., 2011, 2014). In addition, the above-mentioned early alkaline diagenetic environment may also boost the chlorite-coated particles and kaolinite to fill in the pores.

4.2 Diagenetic difference in reservoir sand bodies in various types of cyclic structures

Various structural types of the sequences in the study area have been caused from a combination of factors, such as tectonics, climate, provenance, and the A/S ratio. A previous theoretical model divided the sequence structure into three types with seven sub-types (Zheng et al., 2001). In the study area, upward deepening asymmetric and symmetric cyclic structures are present. In terms of lithologic assemblage and sedimentary succession, the upward-deepening asymmetrical cyclic structure may include the low-accommodation, upward-deepening asymmetrical type and high–accommodation, upward-deepening, asymmetrical types; and the symmetric cyclic structure may include ascending hemicycle-dominated, incompletely symmetrical type, nearly completely to completely symmetrical type and descending, hemicycle-dominated, incomplete symmetrical cyclic structures. Following the distribution of the short-term cyclic structure types in the study area (Zheng et al., 2001), this work mainly focuses on discussion of the diagenetic difference between the following four types of cyclic structures: the high-accommodation, upward-deepening asymmetrical type (hereinafter referred to as A2) (Zheng et al., 2001); the ascending hemicycle-dominated, incompletely symmetrical type (C_1); the nearly completely to completely symmetric type (C_2); and the descending hemicycle-dominated incomplete symmetrical type (C_3). These designations provide help for studies on diagenetic development and evolution, as well as prediction of favorable reservoirs within a small-scale, high-frequency sequence.

4.2.1 Type A_2 sequence

The Type A_2 sequence in the study area was developed in a sedimentary setting with an A/S ratio <1, vertically consisting of obvious base-scouring surfaces, a massive underwater distributary channel sand bodies, and an interdistributary bay (and sometimes thin-bedded underwater natural levees). Lithologically, this sequence consists of pebbly, fine- to moderate-grained sandstones at the base, upward transition to massive moderate to fine-grained sandstones, and thin-bedded siltstones and mudstones in the upper section. As an entirely upward fining sedimentary succession, it was developed during the early MSC1 and early to middle MSC2.

In the Type A_2 sequence of the study area, the massive underwater distributary channel sand bodies have been considered as a favorable reservoir (Zheng et al., 2001), but the Type A_2 during the MSC1 period is somewhat different in diagenesis from that during the MSC2 period. Particles of Type A_2 in the former period proximal to the short-term sequence boundary are in line-embedded contact, with the primary pores mostly destroyed by infilling of a large amount of clay minerals; while those in the latter period proximal to the short-term sequence boundary are in point-line contact, with well-developed primary pores in which dissolved feldspar minerals are found with few quartz microcrystals (Fig. 6).

These conditions indicate that although the Type A_2 sequence during the early MSC1 and that during the early to middle term of MSC2 were both formed in the settings with A/S<1, the main cause for the diagenetic difference lies in the variation in material supply, one of the controls over sequence development. Although the provenance during the early MSC1 provided an adequate material supply, resulting in low-content quartz and a high-content matrix with a low compositional maturity in the detrital compositions of the sandstones (Table 1), corresponding to a poor compression-resistant potential. Poor preservation and the relatively undeveloped secondary pores are indicative of a relatively poor reservoir potential. In comparison, during the early to middle term of the MSC2, the provenance provided abundant material supply, which resulted in high-content quartz and a low-content matrix in the sandstone detrital compositions (Table 1), with a relatively high compositional maturity, corresponding to a high compression-resistant potential and good preservation of the primary pores. Therefore, the reservoir during

the early to middle term of MSC2 is better than that during the early MSC1.

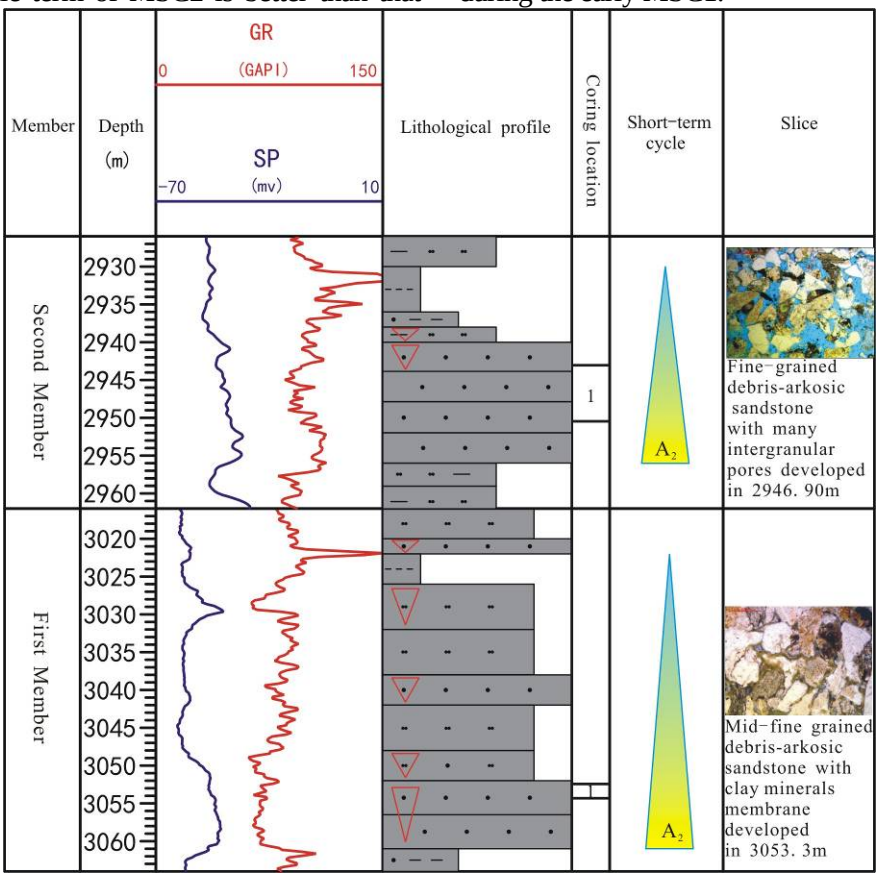

Figure 6. Diagenetic characteristics within Type A_2 of Wells Fudong 11and 051 in the study area

4.2.2 Type C_1 sequence

The Type C_1 sequence in the study area was developed in a sedimentary setting with an A/S ratio >1, vertically consisting of scouring surfaces, thin to moderate underwater distributary channel sand bodies, interdistributary bays, and eustuary bars (distal sand bars). Lithologically, this sequence consists of fine to moderate-grained sandstones-siltstones or argillaceous siltstones-mudstones-siltstones. This succession was mainly developed during the early to middle terms of the three middle term cycles.

As shown in Figure 6, within a short distance from the boundary (0 - 20 m), as the distance from the boundary increases, the number of pores under SEM tends to increase, with increasing dissolution pores. This characteristic is indicative of the control of the boundary over the petrophysical properties of the reservoir sand bodies. Through further observations, it can be found that the carbonate cements (calcite) mostly occur near the boundary, but not prominently.

Clay minerals in the Type C1 sequence of the study area are well-developed. The crossplot of the clay mineral content vs. pore percentage (Fig. 7) shows a correlation between them. The well-developed pores, especially the primary ones, may provide spaces for fluid to flow, which may promote dissolution of such minerals as feldspar and transition between the clay minerals. The presence of a bulk of clay films may somewhat offset compaction of the overburden sediments and slow the decline in porosity, resulting in a porosity-decreasing transition zone (Fig. 8) favorable for preservation of the primary pores. However, it does not mean that the increase in the clay mineral films is better because a large number of clay mineral films may block the pore throats. Only a range in thickness of the films may be favorable for hydrocarbon accumulation.

4.2.3 Type C_2 sequence

The Type C_2 sequence in the study area developed in a sedimentary setting with an A/S ratio >1, vertically consisting of weak scouring surfaces, thin-bedded underwater distributary channel sand bodies, thin-bedded underwater natural levees, interdistributary bays, and distal sand bars (eustuary bars). Lithologically, this sequence consists of fine sandstones-siltstones or argillaceous siltstones-thick-bedded mudstones (containing argillaceous sandstones)-siltstones (sandstone-mudstone interbeds). This succession was mainly developed during the middle phase of the middle term cycle (Fig. 9).

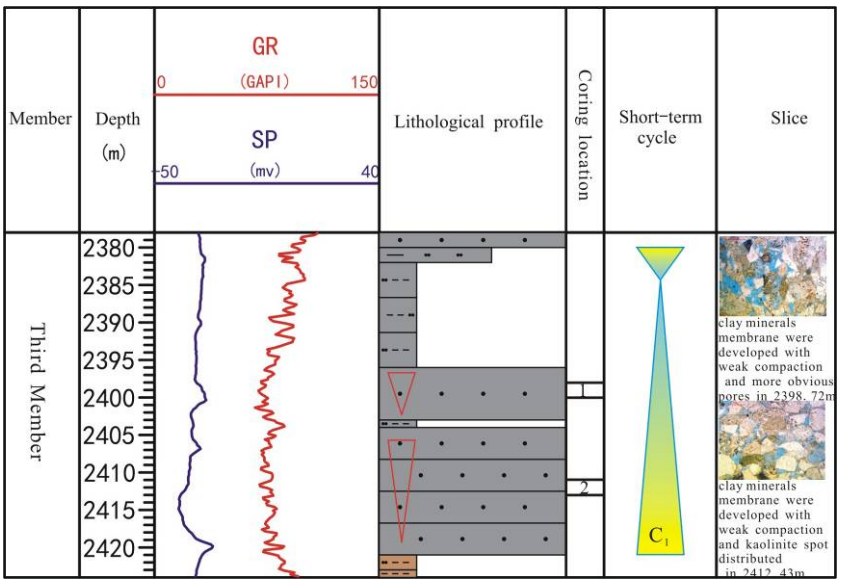

Figure 7. Diagenetic characteristics within Type C_1 of Well Fudong 6 in the study area

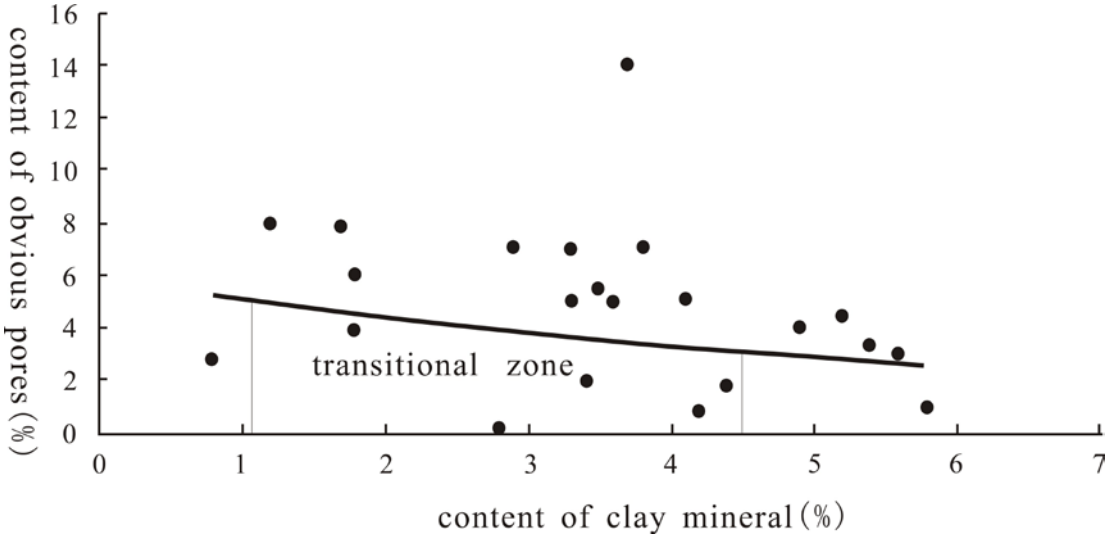

Figure 8. Crossplot between the content of significant porous and clay minerals of Type C_3 in the study area

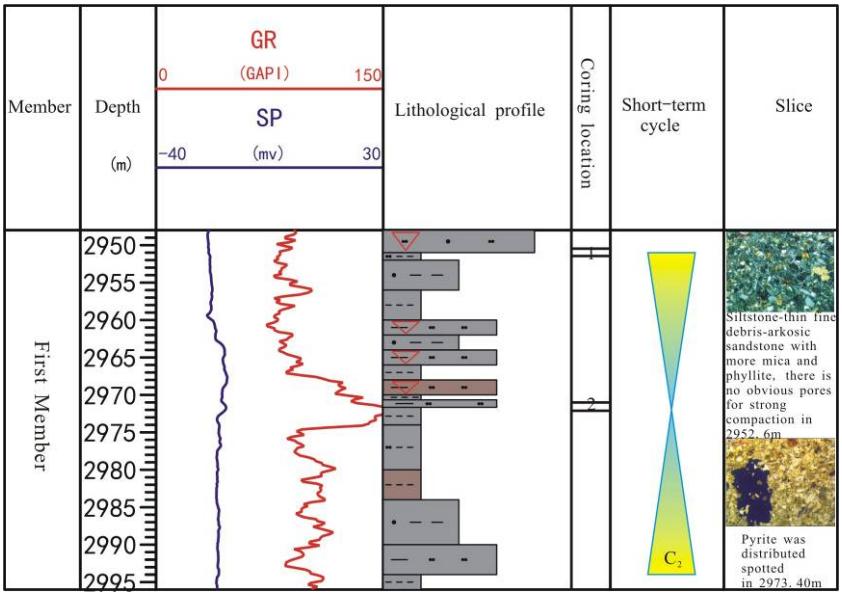

Figure 9. Diagenetic characteristics within Type C_2 of Well Fudong 052 in the study area

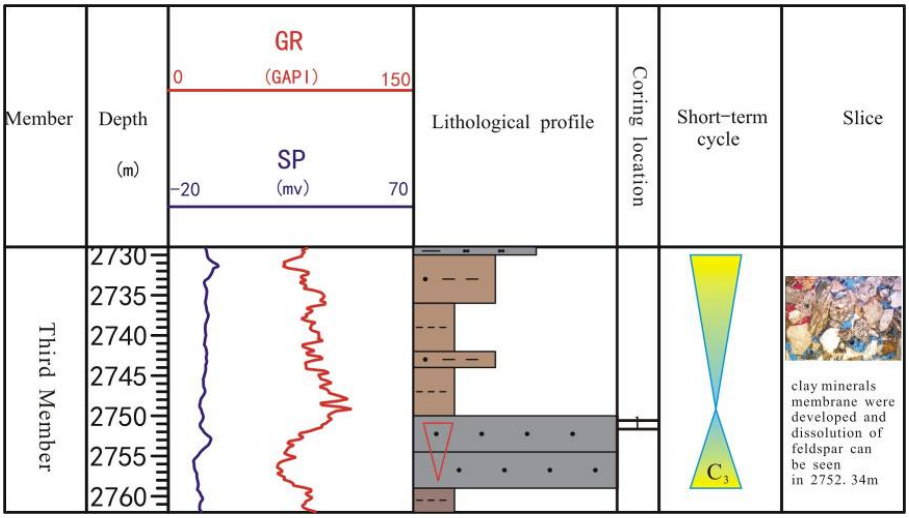

Figure 10. Diagenetic characteristics within Type C_3 of Well Fudong 7 in the study area

The Type C_2 sequence was often developed at the end or edge of the underwater distributary channels, with high-content shale and many plastic lithic particles. By compaction of the overburden sediments, the plastic particles may be deformed and squeezed into the primary pores. This condition is unfavorable for the preservation of the primary pores and deteriorates the reservoir potential (Fig. 9)

4.2.4 Type C_3 sequence

The Type C_3 sequence in the study area was developed in a sedimentary setting with an A/S ratio >1, vertically consisting of scouring surfaces or relative conformities, moderate to thin underwater distributary channel sand bodies or underwater natural levees, inter-distributary bays, and eustuary bars. Lithologically, this sequence consists of fine sandstones or siltstones –mudstones-siltstones (argillaceous siltstones). This sequence was mainly deposited during the late phase of the middle term cycle (Fig. 9).

The Type C_3 sequence in the study area is mainly developed in the transition of the frontal to neritic zone. Due to the lake wave scouring, the estuary bars may be limited to a small scale. Therefore, the reservoir sand bodies may be mostly concentrated in the underwater distributary channel sand bodies in the ascending cycles of the Type C_3 sequence (Fig. 10). Carbonate cements are well developed in the mudstones formed during the ascending datum level. This development may be related to the concentration of salts (rich in Mg^{2+} and Ca^{2+}) in the lake water. However, the increasing carbonate cements may strengthen the compression of the rocks, which may well protect the underwater distributary channel sand bodies deposited during the ascending datum level in a pressure-abnormal environment. In addition, in spite of such a geographical location and a rich argillaceous content in the Type C_3 sequence, a certain control of the scouring lake water over the content of the fine materials and the distribution-limited carbonate cements allow part of the primary pores to be preserved. Meanwhile, the sand bodies and source rocks may be in direct contact, a favorable condition for hydrocarbon accumulation.

4.3 Diagenetic evolution of the reservoir sand bodies in short-term cycles of different key structural types

The analyses of the clay mineral types and their evolutions, as well as vitrinite reflectances (the average value of vitrinite reflectances of 0.5% measured on mudstone samples with vitrinite-rich (72%) and liptinite-poor (24.2%), and low degree of the organic matter measured by Xinjiang Oilfield) of the target reservoirs, indicate that the reservoirs of the Toutunhe Formation in the study area may be in Phase A of the middle-term diagenesis after Phases A and B of the early diagenesis (Yu, 2015). Additionally, the statistics of the production test results of the short-term cycles of the Toutunhe Formation in the Fudong Slope Belt indicate that most of the oil layers may be distributed in SSC4 and SSC7 of MSC2. Therefore, the SSC4 and SSC7 structural types are selected for description of the diagenetic evolution of the reservoir sand bodies in the cycles (Fig. 11).

4.3.1 Short-term cycle SSC4

The short-term cycle SSC4 can be divided into Type A_2 and C_1 structures.

During early diagenesis, the sediments were shallowly buried. Due to physical compaction, the interparticle contact may transit from point-point contact to point-line contact, with the primary pores

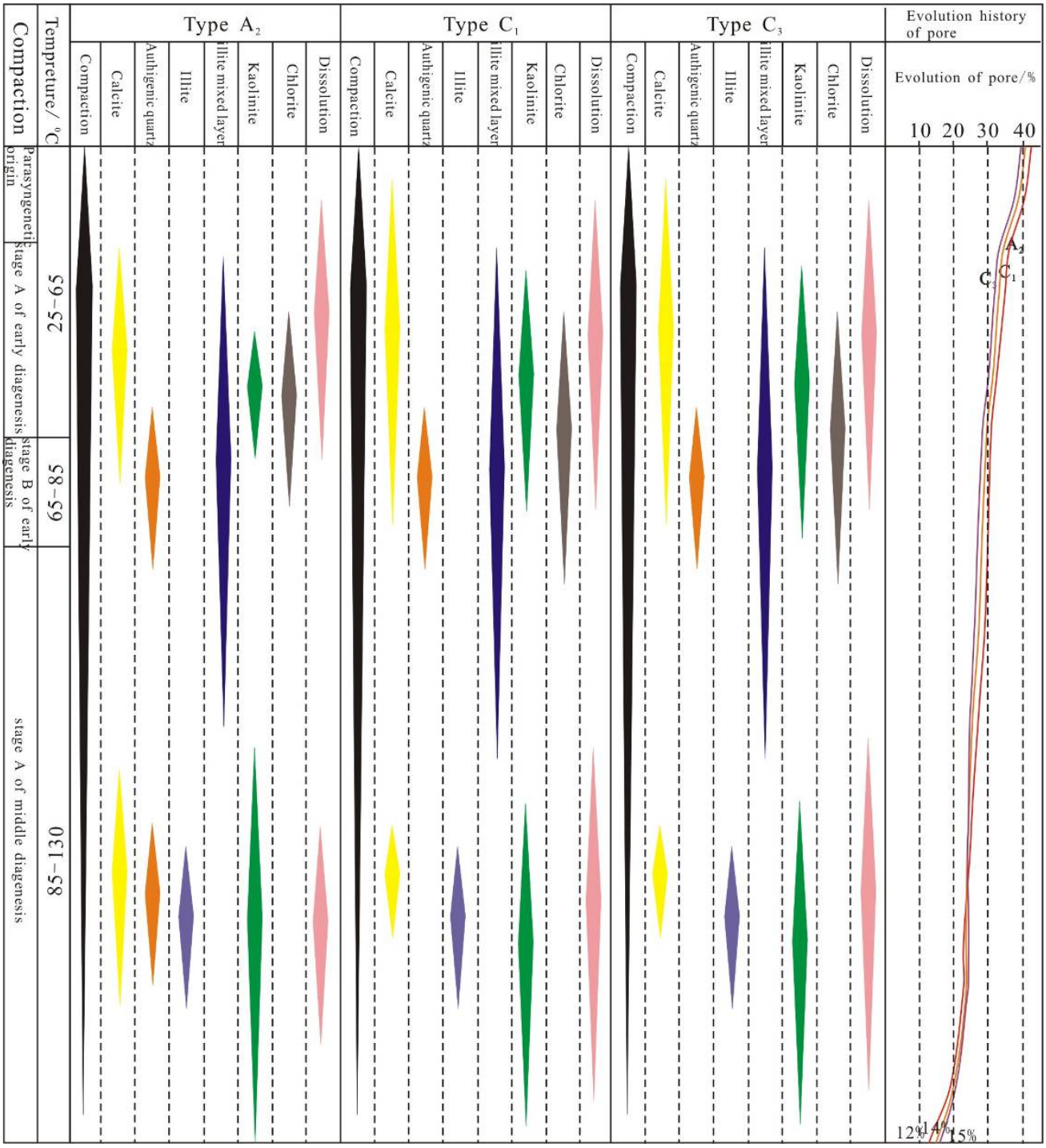

Figure 11 Diagenetic evolution sequence for sandstones in short-term base-level cycles with different structure types

of some plastic minerals greatly destroyed by compressive deformation. In comparison with Type C_1, Type A_2 consists of higher-content quartz and lower-content matrix, indicative of a higher compositional maturity. Additionally, the whole rocks of Type A_2 are more compression-resistant, resulting in better preservation of the primary pores. During the later phase of early diagenesis, the abnormal pressure environment may gradually allow both types of reservoirs to change petrophysically. The mudstone thickness is highly important to the creation of abnormal pressure. The mudstones of Type C_1 are thicker than those of Type A_2, resulting in the reservoir sand bodies of Type C_1 being subjected to pressure by the overburden sediments to a lesser amount than A_2, with less porosity loss. On the other hand, the pores in the reservoirs of the early Type A_2 are better preserved because of the presence of the clay mineral-coated films (mainly as illite-smectite mixture). These films somewhat prevent the porosities from decreasing, but the strong fluid flow is conducive to the development of carbonate cements,

petrophysically destructing the reservoirs. By the early phase of middle-term diagenesis, the development of calcite cements, with less organic acid content, limitedly distributed secondary pores, and extensively developed clay minerals allows the reservoirs of Type A_2 to be petrophysically poorer than those of Type C_1 (Fig. 11).

4.3.2 Short-term cycle SSC7

The short-term cycle SSC7 is dominated by Type C_3.

During early diagenesis, the primary pores were less preserved in the reservoir sand bodies of Type C_3, but the massive mudstones allowed the shallowly buried reservoir sand bodies of Type C_3 to be well preserved in the abnormal pressure environment. On the other hand, the presence of the abnormal pressure inhibited the calcite cements from precipitation and quartz from secondary overgrowth in the sand bodies. The well-developed clay mineral-coated films (mainly as illite–smectite mixture) may inhibit the porosities from decreasing to a certain extent. The dissolution of the acidic fluids during the early phase of middle-term diagenesis may somewhat provide a petrophysical contribution to the reservoir sand bodies of Type C_3, allowing them to be petrophysically better than those of Type C_3 (Fig. 11).

5. CONCLUSIONS

Based on the findings of this work, the following conclusions can be drawn:

(1) Particles below a high-resolution sequence boundary may be in tighter contact than those above the boundary, with lower-content lithic feldspar and higher-content cements, as well as having a greater transition between clay minerals. For example, the transition from the illite-smectite mixture to illite may allow chlorite-coated particles to form and kaolinite to fill in the pores.

(2) Following the distribution of the short-term cyclic structure types in the study area, the Toutunhe Formation consists of four types (A_2, C_1, C_2 and C_3) of cyclic structures. Previous study always focuses on long-term or short-term cyclic structure types of target layers, so this search makes the time-scale of strata analyze more accurate. In different cyclic structure types, reservoir sandbody (underwater distributary channel sand body) has a great difference on petrophysical properties because of different diagenesis effect. So make analysis on diagenesis in different short-term cyclic structure types can provide a basis for rough prediction of subtle reservoirs.

(3) The underwater distributary channel sand bodies of Type A_2 are dominated by mechanical compaction. Due to the difference in detrital composition, the underwater distributary channel sand bodies in Type A_2 of MSC2 are much better than those of some other types. The underwater distributary channel sand bodies of Type C_1 are characterized by weak compaction, local carbonate cementation, and well-developed clay minerals. Because of a coupling relationship between the development of the primary pores and the content of clay minerals, the underwater distributary channel sand bodies of Type C_1 have good petrophysical properties. In comparison, those of Type C_2 present reservoirs with poor petrophysical properties, owing to fine particles with a weak compaction-resistant potential, and those of Type C_3 are characterized by a strong compaction-resistant potential and limitedly distributed carbonate cements. These characteristics may result in good preservation of the primary pores in the sand bodies that is favorable for oil and gas accumulation.

(4) The short-term cycles in SSC7 of Type C_1 and in SSC4 of Type C_3 exhibit constructive diagenesis in which the underwater distributary channel sand bodies represent the most favorable reservoirs. The short-term cycle SSC4 of Type A_2 exhibits both constructive and destructive diagenesis in which the underwater distributary channel sand bodies represent good reservoirs.

Acknowledgement

For their financial support, the author gratefully acknowledges the Talent Introduction Project performed by the Karamay campus of the China University of Petroleum (Beijing) (No. RCYJ2016B-01-010) and the fund for Young Teachers' Scientific Research of College Scientific Research Program in Xinjiang Uygur Municipality (No. 20160621220132602).

References

Ahmed A., Ali Y, Mohamed A.E. & Asmaa A. 2016. *Structures and sequence stratigraphy of the Miocene successions, southwestern Gulf of Suez, Egypt*. Original research article, 7(5):821-834.

Alexandre P., Guilhem H., Jean-Paul C. & **Jean-Claude R.** 2016. *Diagenesis of Oligocene continental sandstones in salt-walled mini-basins—Sivas Basin, Turkey*. Original research article, 339(11):13-31.

Álvaro R.B., Ana M.A.Z. & Rebeca M.G. 2017. *Diagenesis of continental carbonate country rocks underlying surficial travertine spring deposits*. Original research article, 437(A):4-14.

Andrew P.R. 2015. *Magnetic mineral diagenesis*. Earth-Science Reviews, 151:1-47.

Cao G., Wang X., Zhu X., Qu Q., Wu B., He J. & Dai B. 2016. *Diagenesis Evolution of Esx3Nearshore subaqueous Fan Reservoir and Its influence on*

property in the Steep Slope Zone of Western Chezhen Sub-sag. Acta Sedimentologica sinica，34(1):158-167.

Cao Y., Cheng X., Wang Y. & Ma B. 2015. *Diagenesis of Paleogene Glutenite Reservoir and Its Physical Property in the North Zone of Chezhen Sag.* Acta Sedimentologica sinica，33(6):1192-1203.

Fernando J.G. & Ricardo A.A. 2015. *Sedimentology and sequence stratigraphy from a mixed (carbonate–siliciclastic) rift to passive margin transition: The Early to Middle Cambrian of the Argentine Precordillera.* Original research article,316(1):39-61.

Han D.L., Zhang Ch.M. & Yin T.J. 2010. *Diagenetic reaction pattern of the sequence boundary and its impacts on reservoir quality.* Oil & Gas Geology, 31(4):449-454.

Higgs K.E., King P.R., Raine J.I., Sykes R., Browne G.H., Crouch E.M. & Baur J.R. 2012. *Sequence stratigraphy and controls on reservoir sandstone distribution in an Eocene marginal marine-coastal plain fairway, Taranaki basin, New Zealand.* Marine and Petroleum Geology, 32(1):110-137.

Hilda C.G.P., Octavian C. & Ulises H.R. 2017. *Sequence stratigraphy of the Miocene section, southern Gulf of Mexico.* Marine and Petroleum Geology, 86:711-732.

Lai J., Wang G.W., Wu D.Ch., Cao J.N., Zhang X.T., Ran Zh., Yao Y.B. & Zhang Y.D. 2014. *Diagenetic facies distribution in high resolution sequence stratigraphic framework of Chang 8 Oil Layers in the Jiyuan area.* Geology in China，41(5):1487-1502.

Liu N., Wen H.G., Yu J.W. & Qi L.Q. 2014. *Analysis of Macroscopic Heterogeneity within High Resolution Sequence Stratigraphic Framework in Toutunhe Formation of Middle Jurassic in East of Fukang Slope Zone，Junggar Basin.* Geological Review, 60(5):1158-1166.

Lu B., Zhang J., Li T. & Lu M.A. 2008. *Analysis of Tectonic Framework in Junggar Basin.* Xinjiang Petroleum Geology, 29(3):283-289.

Mctavish R.A. 1978. *Pressure retardation of vitrinite digenesis, offshore north-west Europe.* Nature, 271(16): 648-650.

Morad S., Al-Ramadan K., Ketzer J.M. & De Ros L.F. 2010. *The impact of diagenesis on the heterogeneity of sandstone reservoirs: a review of the role of depositional facies and sequence stratigraphy.* AAPG Bulletin, 94(8):1267-1309.

Qi L.Q., Qian Y.X., Wang L., Li C.L., Wen H.G. & Yu J.W. 2014. *Characteristics of base-level cycles and sand body distribution of Toutunhe Formation in Fudong slope zone, Junggar Basin, China.* Journal of Chengdu University of Technology (Science & Technology Edition), 41(2):136-144.

Soreghan G.L., Bralower T.j., Chandler M.A., Kiehl J., Lyle M., Lyons T.W., Maples C.G., Montanez I.P. & Otto-Bliesner B L. 2005. *GeoSystems：Probing Earth's Deep-Time Climate & Linked System.* Arlington, VA：Report of a workshop sponsored by the National Science(NSF):35.

Vail P.R., Audemard F. & Bowman S.A. 1991. *The stratigraphic signatures of tectonics, eustasy and sedimentology: Cycles and evens in stratigraphy.* AAPG Bulletin, 11(3):617-659.

Yu J.W. 2015. *Sequence and seismic sedimentology analysis of Toutunhe Formation in Fudong Slope area of Junggar basin.* Chengdu University of Technology.

Yu J.W., Ren W., Wang W.X., Wang Z.Sh., Liu N. & Ouyang X.Q. 2015**.** *Formation Mechanism of Toutunhe Abnormal Pressure of Middle Jurassic in Fudong Slope Area, Junggar Basin.* Xinjiang Petroleum Geology, 36(5):521-525.

Yu J.W., Zheng R.C., Qi L.Q., Zhang Z.B., Wen H.G. & Li Y. 2014. *Precise Analysis on High-resolution Sequence Stratigraphy and Micro-facies of Toutunhe Formation of Middle Jurassic in the East Slope Zone, Fukang Sag,Junggar basin.* Geologic Review, 60(6):1337-1347.

Zhang K.X., Bai G.P., Jing F.M. & Wang Q. 2016. *Diagenesis in sequence stratigraphical framework: a case study of sandstone of Member 3 of Shahejie Formation in the south-central Raoyang sag.* Acta Petrolei Sinca, 37(6):728-742.

Zheng R.C., Peng J. & Wu Ch.R. 2001. *Grade Division of Base-Level Cycles of Terrigenous Basin and Its Implications.* Acta Sedimentologica Sinic, 19(2):249-255.

Zhu Sh.F., Zhu X.M., Wang X.L. & Liu Zh.Y. 2011. *Zeolite diagenesis and its control on petroleum reservoir quality of Permian in northwestern margin of Junggar Basin. China.* Sci China Earth Sci, 41(11):1602-1612.

Zhu Sh.F., Zhu X.M., Wu D., Liu Y.H., Li P.P., Jiang Sh.X. & Liu X.Ch. 2014. *Alteration of volcanics and its controlling factors in the Lower Permian reservoirs at northwestern margin of Junggar Basin.* Oil & Gas Geology, 35(1):77-78.

Received at: 29. 12. 2017
Revised at: 09. 04. 2018
Accepted for publication at: 02. 04. 2018
Published online at: 14. 05. 2018